Message Passing and Hierarchical Models for Simultaneous Tracking and Registration

Message Passing and Hierarchical Models for Simultaneous Tracking and Registration

David Cormack, *Student Member, IEEE* and James R. Hopgood, *Member, IEEE*

Abstract

Sensor registration is an important problem that must be considered when attempting to perform any kind of data fusion in multi-modal, multi-sensor target tracking. In this Multiple Target Tracking (MTT) application, any inaccuracies in the registration can lead to false tracks being created, and tracks of true targets being stopped prematurely. This article introduces a method for simultaneously tracking multiple targets in a surveillance region and estimating appropriate sensor registration parameters so that sensor fusion can be performed accurately. The proposed method is based around particle Belief Propagation (BP), a recent but highly efficient framework for tracking multiple targets. The proposed method also uses a hierarchical model which allows for multiple processes to be linked and interact with one another. We present a comprehensive set of simulations and results using differing, asynchronous sensor setups, and compare with a Random Finite Set (RFS) approach, namely the Sequential Monte Carlo (SMC)-Probability Hypothesis Density (PHD) filter. The results show the proposed method is 17% more accurate than the RFS approach on average.

Index Terms

Message passing, belief propagation, PHD filter, multiple target tracking, sensor registration, sensor fusion, radar, camera

I. Introduction

A. Problem Outline

It is now more important than ever to maintain ground and airborne surveillance around key locations and assets. By using a diverse range of sensing modalities to track multiple targets, sensor fusion performance can be increased, and spatio-temporal uncertainty can be reduced [1]. Consider, for example, the scenario shown in Fig. 1 where two radars (A and B) observe a common surveillance region from fixed and known locations. Using this sensor configuration, the cross-range uncertainty in one radar can be reduced by exploiting the down-range uncertainty

This work was supported by the Engineering and Physical Sciences Research Council (EPSRC) Grant number EP/S000631/1 and the MOD University Defence Research Collaboration (UDRC) in Signal Processing.

The work of D. Cormack is supported by Leonardo MW Ltd., Edinburgh, EH5 2XS, U.K.

D. Cormack is with the School of Engineering and Physical Sciences, Heriot-Watt University, Edinburgh, EH14 4AS, U.K. (email: drc9@hw.ac.uk)

J.R. Hopgood is with the Institute for Digital Communications, University of Edinburgh, Edinburgh, EH9 3FG, U.K. (email: james.hopgood@ed.ac.uk)

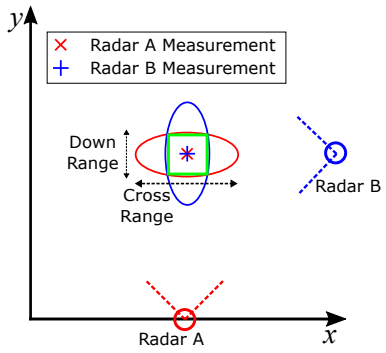

Fig. 1. Uncertainty reduction using two radars, with their field-of-view (FoV) shown in dotted lines facing a common target, at approximately 90° to one another. The down-range uncertainty in Radar A can reduce the cross-range uncertainty of Radar B and vice-versa.

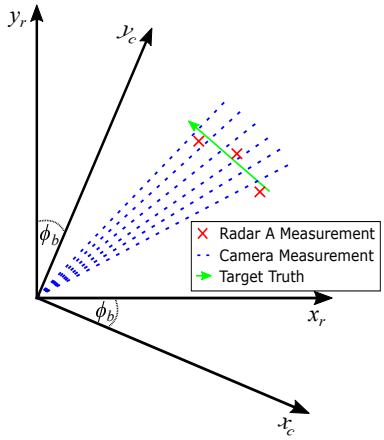

Fig. 2. An overview of the faster track-update-rate available if heterogeneous sensors are used. Between successive radar detections on the same target, angular data from camera images can be used to update track estimates more frequently. There may be an unknown rotation ϕ_b between the radar and camera frame of reference that will need to be overcome.

in the other and vice-versa. The main advantages of using radar include accurate target detection and localisation, and its ability to scan large volumes of space in a short period of time [2]. The use of cameras alongside radar can help improve angular accuracy further, as they often provide more accurate angular measurements at a much faster update rate, albeit in a reduced scanning area (see Fig. 2). The frames of reference of the two sensors may not align however; there may be a rotational offset or bias that needs to be overcome before data fusion can occur.

Sensors that are deployed as a part of larger fusion system are not often developed specifically for data fusion; they are often commercial off-the-shelf (COTS) devices and would normally operate individually. Further development and implementation is required to allow fusion to be performed between them. COTS sensors are likely to operate asynchronously, and in their own frame of reference (FoR), making the fusion problem more challenging. This work focuses on the registration problem with asynchronous sensors, where there may be relative biases or unknown offsets between each of the individual frames of reference. In our homogeneous scenario in Fig. 3(a), there are relative registration errors in both range r_b and azimuth ϕ_b between the two radars. For the heterogeneous setup

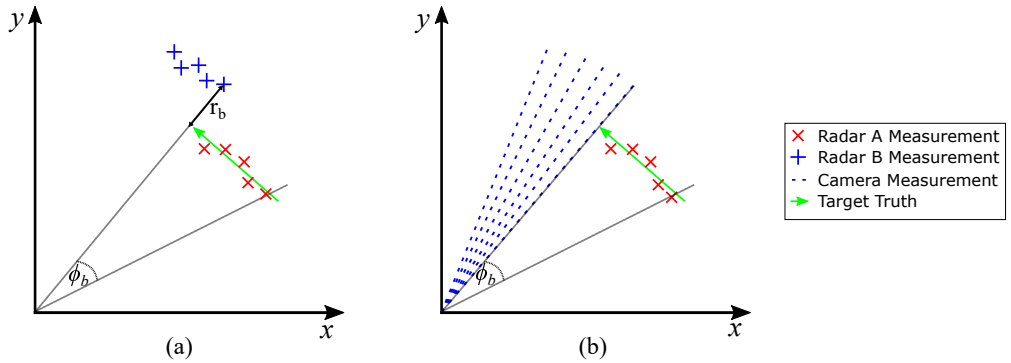

Fig. 3. Examples of the sensor registration problem for simple two-dimensional cases. (a) A homogeneous network containing two radars, with range bias r_b and azimuth bias ϕ_b. (b) A heterogeneous network where Radar B has been replaced with a camera that has azimuth registration bias ϕ_b. All of these biases must be estimated and accounted for during the fusion process.

in Fig. 3(b), there is a relative angular error ϕ_b between the radar and the camera. At times, it may be impossible to register the full system correctly to a global FoR (eg. WGS84, J2000) where GPS and other navigation systems may be denied.

B. Proposed Method and Contributions

This work presents a hierarchical Bayesian method for simultaneously estimating the states of multiple targets along with the appropriate registration parameters. This hierarchical model has been applied to a number of problems previously, such as Simultaneous Localisation and Mapping (SLAM) [3], sensor drift estimation [4], and also to false alarm rate estimation [5]. The main advantage of using this type of approach is the plug-and-play architecture that the hierarchical model provides. Any Multiple Target Tracking (MTT) algorithm could, in theory, be implemented within the hierarchy, as long as a suitable parameter likelihood has been derived to link the two processes together. Another key advantage of the proposed technique is the capability of registering relative sensor frames correctly, without alignment or knowledge of a global FoR. Moreover, this work deals with extrinsic parameter estimation, such as sensor orientation and location, but could be extended or redeveloped to estimate system parameters [6], [7] such as the probability of target detection for example.

In this article, we consider centralised fusion scenarios where the fusion engine or centre has access to all of the raw measurements from the sensors. As a result of this, each sensor does not perform its own local tracking routine before sending information to the centre. All measurements are kept in their polar representation and do not need to be converted. The sensors that are present are assumed to be COTS sensors which operate asynchronously and make the registration problem more challenging. This is likely to be the case in practice; sensors are very rarely synchronised fully.

This work provides a novel extension of Message Passing (MP) MTT algorithms to allow for simultaneous registration and sensor fusion. The two main novel contributions of this article are:

1) development of a MTT technique based on MP that incorporates sensor calibration in a joint manner, in contrast to existing techniques which solve tracking and calibration separately by using pseudo-measurements

[8], [9]; our proposed technique also resolves the data association problem efficiently using MP algorithms [10];

2) the derivation of a suitable sensor parameter likelihood for the particle Belief Propagation (BP) implementation.

This article also includes a comprehensive set of simulations (Section VI) involving the sensor setups and biases shown in Fig. 3. Moreover, the simulations shown in this article consider a similar range bias compared to those simulated in [8], [11], however the azimuth bias simulated here is an order of magnitude larger. A full comparison with a Probability Hypothesis Density (PHD) approach [12] is also provided.

This article extends our previous journal publication [12] by showing it is possible to combine a vector-type tracking method [13], with the hierarchical model inspired by the set-type tracking literature. The two conference articles that we have previously published on this topic [14], [15] contained preliminary results. This article provides a lot more detail on the theory, results and analysis, and describes the specific implementation details of our algorithm.

The rest of the article is organised as follows: Section II contains a literature review of existing techniques for resolving sensor registration; Section III defines the registration and fusion problems and provides an overview of the algorithms that are used. Section IV introduces the necessary parameter likelihood functions that are used to estimate the registration parameters, with appropriate performance metrics provided in Section V. Simulations and results are shown in Section VI and conclusions are drawn in Section VII.

II. Background and Motivation

A. State-of-the-Art in Sensor Registration

Target tracking systems are typically based on dynamical models and sensor observation models, which need to be carefully tuned to give a suitable output [16]. Ideally, real-world systems should be calibrated accurately using parameter estimation [17] before being deployed out in the field. If the registration parameters are not correctly estimated, the projection of sensor measurements into a common FoR will be incorrect. This may make measurements appear distant from one another, which in turn may make false tracks appear, and prematurely stop correct tracks. Sensor biases could come from different sources, and manifest themselves in different ways. Bias sources could include misalignment during installation, harsh weather, or strong platform vibrations e.g. high winds, aircraft take-off and landing etc. With dynamic platforms such as aircraft, there are no guarantees that the bias will remain static throughout the scenario, or stay in its pre-calibrated state, hence the need for this type of online registration algorithm that can continually account for potentially dynamic and time-varying registration parameters. Having this type of algorithm available would remove the burden from the system operator of having to continually realign sensors and avoid a loss in tracking accuracy due to incorrect data fusion.

Previous works in the field of radar and camera fusion [18], [19] have shown the benefits of exploiting multiple sensors to improve accuracy and update rates. However, these articles either omit the registration problem altogether, or perform the sensor registration before fusion occurs. Performing sensor registration in this way could lead to further systematic biases in the system. Methods for resolving registration errors have been presented in [8], [9] which attempt to resolve the errors using pseudomeasurement approaches. Such approaches often reduce the problem down

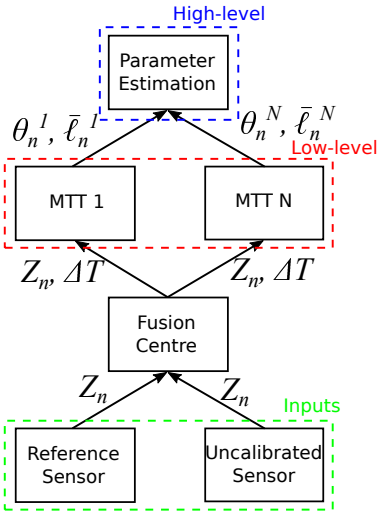

Fig. 4. Flowchart of the simultaneous tracking and registration process. Asynchronous measurements are sent to the fusion centre when ready, and then used in the low-level process for tracking. When measurements are received from the uncalibrated sensor, the parameter likelihood $\bar{\ell}_n^i = \bar{\ell}_n(q_n^i|\mathbf{z}_n)$ is calculated to update the appropriate registration parameter(s) in the high-level process (see Section III-A).

to pairs of sensors, with estimated target states and unknown biases placed into a stacked vector. Other approaches such as [20], [21] use machine learning algorithms and neural networks to determine appropriate parameters. One of the main drawbacks to machine learning methods is that they require very large amounts of training data to give accurate results and, in turn, take a long time to train before testing and deployment is possible [22], [23]. Works such as [24], [25] focus on the sensor localisation and distributed fusion problems, where all sensors perform their own individual tracking routines. The filtered distributions are then shared between pairs of sensors to perform fusion, and to solve the localisation problem. These works also assume that each sensor can perform its own target tracking accurately, which may not be the case in this article.

B. State-of-the-Art in Multi-Target Tracking (MTT)

The hierarchical model used in this work is shown in Fig. 4, and will be discussed in depth in Section III. This two-stage model is very flexible and allows for many design choices to be made such as the parameters to be estimated, models that describe how the sensor registration is expected to evolve, and the MTT algorithm used in the low-level stage of this plug-and-play architecture. Various types of tracking algorithm could be used in the low-level process for MTT including vector-type approaches such as Joint Probabilistic Data Association (JPDA) [26] and Multiple Hypothesis Tracking (MHT) [27], [28], or set-type approaches such as the PHD filter [29], [30], the Cardinalized Probability Hypothesis Density (CPHD) filter [31] and labelled Random Finite Set (RFS) methods [32], [33]. This article will use an approach based on BP and MP techniques [13], [34]. These techniques for MTT have seen a recent revival in the literature and bring a number of advantages, such as scalability to larger tracking scenarios; the complexity only scales quadratically in the number of targets, and linearly in the number of measurements per sensor. Fundamental tracking algorithms such as the Kalman filter [35] and the particle filter

[36] can be seen as instances of the Sum-Product Algorithm (SPA). The SPA is very efficient in computing the marginal posterior probability density functions (pdfs) [37].

Bayesian tracking methods require the posterior pdfs $f\left(\mathbf{x}_{n,k} \mid \mathbf{z}_{1:n}\right)$, which are the marginals of the joint posterior pdf $f\left(\mathbf{x}_{n} \mid \mathbf{z}_{1:n}\right)$, where $\mathbf{x}_{n,k}$ represents a state vector of target k, $\mathbf{x}_{n} = [\mathbf{x}_{n,1}, \ldots, \mathbf{x}_{n,K}]^{T}$ represents a state vector for all targets at time n, and $\mathbf{z}_{1:n}$ represents the sensor measurements from time-step 1 to n. By using the SPA, the marginal pdfs can be calculated much faster than when using direct marginalisation. This advantage alone makes the SPA better suited than other traditional MTT algorithms for larger problems involving many sensors and targets.

The MTT problem is made more difficult by the data association (DA) problem; the sensors and filters do not know which received measurement corresponds to each target. Classic solutions to this problem include the Hungarian algorithm [38], Auction [39], or MHT algorithms [27], [40]. For this work, we use a more recent association algorithm called the Sum-Product Algorithm for Data Association (SPADA) [10], which is also based on MP and the SPA. By making distinct associations between measurements and targets, track histories can be stored and full target trajectories could be given as an output to system operators.

C. Proposed Method

The problem is broken down into two separate layers as shown in Fig. 4. The high-level process will estimate the registration parameter(s), and the low-level process will estimate the multiple target states using techniques such as those described in Section II-B, based on the estimated parameter(s). This article presents a novel approach to estimating sensor registration parameters using message passing and hierarchical models in both homogeneous and heterogeneous sensor setups. This method tracks multiple targets in the surveillance region, while estimating appropriate parameters so that sensor measurements are correctly projected onto a common frame of reference. The measurements used for performing the parameter estimation will come from the uncalibrated sensor which will detect the non-cooperative targets in the surveillance region. So, for example, the uncalibrated sensor in Fig. 3 could either be Radar B or the camera, with the calibrated sensor being Radar A.

For tracking targets in the low-level process, the main focus will be on MP algorithms, specifically a SPA-based reformulation of the Joint Integrated Probabilistic Data Association (JIPDA) filter [34], [41]. This technique comes into the category of vector-type tracking methods, where target states and measurements are represented as random vectors [28]. The algorithm will be implemented using particle BP, meaning that each individual target, belief and message will be represented by a particle distribution. The use of particles allows for non-linear, non-Gaussian models to be dealt with directly, making this an attractive choice for dealing with radars and cameras. This implementation will be compared to one containing a Sequential Monte Carlo (SMC)-PHD filter which, in contrast, is a set-type tracking method where targets and measurements are represented as RFSs. Both of these MTT algorithms can be directly integrated into the low-level of the hierarchical model using a suitable filter-specific parameter likelihood [42] which acts as a measure of the accuracy of the high-level process.

III. Problem Definition

The main challenges associated to this work are highlighted in Fig. 3. All of the biases must be estimated simultaneously with the multiple target states. First, consider the scenario shown in Fig. 3(a) containing multiple radars. Here, the range-azimuth measurements from Radar B have been projected into the Radar A FoR, with potentially time-varying registration errors $q_n = [r_{b,n}, \phi_{b,n}]^T$. It is only when the measurements are in a common frame that the registration errors are apparent.[1] The same applies to the scenario in Fig. 3(b), where Radar B has been replaced with a camera to improve the update rate between the sensors. The camera only provides azimuth measurements, and target range cannot be resolved in this case using a single passive sensor. In this scenario, there is a relative angular bias $q_n = \phi_{b,n}$. The following sections will provide more detailed information on the problems being solved.

A. Sensor Registration

The high-level process will estimate the potentially time-varying sensor registration configuration q_n at time n in each of the scenarios. The densities associated with the high-level process will be denoted with $\bar{\cdot}$ for the remainder of the article. A typical Bayesian recursion is used to propagate the posterior density, $\bar{p}_n(q_n)$, of the registration configuration such that in its general form

$$\bar{p}_{n|n-1}(q_n|\mathbf{z}_{n-1}) = \int_S \bar{f}_{n|n-1}(q_n|q')\bar{p}_{n-1}(q'|\mathbf{z}_{n-1})\mathrm{d}q', \tag{1a}$$

$$\bar{p}_n(q_n|\mathbf{z}_n) = \frac{\bar{\ell}_n(q_n|\mathbf{z}_n)\bar{p}_{n|n-1}(q_n|\mathbf{z}_{n-1})}{\int_S \bar{\ell}_n(q'|\mathbf{z}_n)\bar{p}_{n|n-1}(q'|\mathbf{z}_{n-1})\mathrm{d}q'}. \tag{1b}$$

where $\bar{f}_{n|n-1}(q_n|q')$ is a first-order Markov process representing the expected change in sensor registration in time, and $\bar{\ell}_n(q_n|\mathbf{z}_n)$ is the sensor parameter likelihood, discussed in Section IV.

As described earlier, the registration configuration q_n will be represented using a particle distribution q_n^i for $1 \leq i \leq N$, where each i represents a different configuration. Each individual particle is weighted with w_n^i and has a corresponding set of underlying MTT statistics θ_n^i that are dependent on the choice of algorithm used in the low-level process. More on these statistics can be found in [43]. The high-level process is flexible, and allows for the particle states to be fixed to a preset grid [44], or allowed to move with a resampling process to search the wider space [45].

[1]The true target trajectory is located in a world reference frame e.g. WGS84, but for simplicity, it is assumed that the Radar A FoR is perfectly aligned to this.

With this particle representation, equations (1) become:

$$\bar{p}_{n|n-1}(q_n|\mathbf{z}_{n-1}) = \sum_{i=1}^{N} w_{n|n-1}^{i}\ \delta(q_n - q_n^i), \tag{2a}$$

$$\bar{p}_{n}(q_n|\mathbf{z}_{n}) = \sum_{i=1}^{N} w_{n}^{i}\ \delta(q_n - q_n^i), \tag{2b}$$

$$w_{n|n-1}^{i} = \sum_{j=1}^{N} w_{n-1}^{j}\ \bar{f}_{n|n-1}(q_n^i|q_{n-1}^j), \tag{2c}$$

$$w_{n}^{i} = \frac{w_{n|n-1}^{i}\ \bar{\ell}_n^i}{\sum_{j=1}^{N} w_{n|n-1}^{j}\ \bar{\ell}_n^j} \tag{2d}$$

where $\bar{\ell}_n^i = \bar{\ell}_n(q_n^i|\mathbf{z}_n)$ is the sensor parameter likelihood evaluated for particle i. This routine is performed after the MTT in the low-level process has been completed. After updating the high-level weights $w_n^i, i = 1, \ldots, N$, *particle degeneracy* is tested for using the effective sample size [36, Eq.(51)]. Degeneracy can occur after a number of time-steps, where all of the weight will be placed on one particle, and the rest of the particle weights will be negligible. This implies that much of the computational effort is being used on configurations that are highly unlikely. If the effective sample size is below a threshold τ_r, stratified resampling [46] is performed on the particles to increase their spread in the high-level state space. This choice of stratified resampling over other traditional methods in this application is justified due to the shape of the updated likelihood: this distribution tends to be very sharp and peaky around the true value. Small errors in azimuth make the tracking accuracy much worse, and therefore reduces the parameter likelihood and output likelihood. In resampling, particles with high weights are statistically chosen much more often and it is possible that the samples could all collapse down to one point in the state space which is known as *particle impoverishment*. By using stratified resampling, the variance of the newly-drawn particles should be kept larger and the problem can be avoided [46].

B. MTT and Fusion

Multiple Target Tracking (MTT) estimates the states of multiple targets using only the measurements from one or more sensors, even where the number of targets is unknown and time-varying. The target states often contain information on a target's position and velocity, but the state could be extended to incorporate more variables if required. The low-level process in the hierarchy estimates the potentially time-varying multi-target state, $\psi_n \in \mathcal{X}^{m_n}$, which is conditional on the sensor configuration q_n. This MTT process evolves with a Markov transition function $f_{n|n-1}(\psi_n|\psi_{n-1})$ which for this article will be a near-constant velocity (NCV) model [47]. Similar to the high-level process in Equation (2), a Bayes recursion is used to propagate the joint posterior of the MTT process:

$$p_{n|n-1}(\psi_n|q_n, \mathbf{z}_{n-1}) = \int_{\Psi} f_{n|n-1}(\psi_n|\tilde{\psi}) p_{n-1}(\tilde{\psi}|q_n, \mathbf{z}_{n-1}) \mathrm{d}\tilde{\psi} \tag{3a}$$

$$p_{n}(\psi_n|q_n, \mathbf{z}_{n}) = \frac{\ell_n(\psi_n|q_n, \mathbf{z}_n) p_{n|n-1}(\psi_n|q_n, \mathbf{z}_{n-1})}{\int_{\Psi} \ell_n(\tilde{\psi}|q_n, \mathbf{z}_n) p_{n|n-1}(\tilde{\psi}|q_n, \mathbf{z}_{n-1}) \mathrm{d}\tilde{\psi}} \tag{3b}$$

where $\ell_n(\psi_n|q_n, \mathbf{z}_n)$ is the multi-measurement/multi-target likelihood, which describes the association likelihood between measurements and targets.

Many MTT algorithms give good tracking accuracy, but they can become computationally cumbersome when the system model becomes larger in terms of the number of sensors and targets. MTT methods with lower complexity and better scalability can be derived and implemented using BP, also known as MP or the SPA [13]. The SPA gives a close approximation to Bayesian inference and allows for a suitable trade-off between accuracy and computation time. The final implementation can be structured in such a way that non-linear dynamical and measurement models can be overcome, along with an unknown and time-varying number of targets [34].

C. Model Definitions

1) Dynamical Model: The measurement buffer will have access to the raw range-bearing radar measurements and/or the bearing-only camera measurements that are recorded at a given iteration n and physical time t_n. The MTT routine will be performed using $4-D$ Cartesian state vectors with elements

$$\mathbf{x}_{n,k} = [x_{n,k}\ \dot{x}_{n,k}\ y_{n,k}\ \dot{y}_{n,k}]^T \tag{4}$$

where $x_{n,k}, y_{n,k}$ are the x and y positions of target k at time n and $\dot{x}_{n,k}, \dot{y}_{n,k}$ are the x and y velocities of the target. The collection of $\mathbf{x}_{n,k}$ vectors make up the multi-target state $\psi_n = [\mathbf{x}_{n,1}, \ldots, \mathbf{x}_{n,K}]^T$. It is assumed that each and every target follows a NCV model [16], [47], which is a common model used in MTT. Other state-space motion models can also be used in this framework. The NCV model is given by

$$\mathbf{x}_{n,k} = \mathbf{F}_n \mathbf{x}_{n-1,k} + \mathbf{w}_{n,k} \tag{5}$$

where $\mathbf{F}_n$ is the state transition matrix

$$\mathbf{F}_n = \begin{bmatrix} 1 & \Delta_n & 0 & 0 \\ 0 & 1 & 0 & 0 \\ 0 & 0 & 1 & \Delta_n \\ 0 & 0 & 0 & 1 \end{bmatrix},\ \Delta_n = t_n - t_{n-1}, \tag{6}$$

and $\mathbf{w}_{n,k}$ represents zero-mean white Gaussian process noise with covariance

$$\mathbf{Q}_n = \begin{bmatrix} u\Delta_n^3/3 & u\Delta_n^2/2 & 0 & 0 \\ u\Delta_n^2/2 & u\Delta_n & 0 & 0 \\ 0 & 0 & u\Delta_n^3/3 & u\Delta_n^2/2 \\ 0 & 0 & u\Delta_n^2/2 & u\Delta_n \end{bmatrix} \tag{7}$$

and u is the acceleration noise value in both the x and y directions.

2) Radar Measurement Model: This is defined as

$$\mathbf{z}_{n,k}^R = h^R(\mathbf{x}_{n,k}) + \eta_{n,k}^R, \tag{8}$$

with

$$h^R(\mathbf{x}_{n,k}) = \begin{bmatrix} r_{n,k} \\ \phi_{n,k} \end{bmatrix} = \begin{bmatrix} \sqrt{x_{n,k}^2 + y_{n,k}^2} \\ \tan^{-1}(x_{n,k}, y_{n,k}) \end{bmatrix}, \tag{9}$$

where $r_{n,k} > 0$, $\tan^{-1}(x_{n,k}, y_{n,k})$ is the four-quadrant inverse tangent function, and the resulting $\phi_{n,k}$ lies within $[0, 2\pi)$. The additive noise term $\eta^R_{n,k}$ is defined by

$$\eta^R_{n,k} \sim \mathcal{N}(\eta^R_{n,k}; \mathbf{0}, \text{diag}(\sigma^2_{r_\text{r}}, \sigma^2_{\phi_\text{r}})) \tag{10}$$

where σ_{r_r} and σ_{ϕ_r} are the radar's range and azimuth standard deviations respectively.

3) Camera Measurement Model: This is described by

$$\mathbf{z}^C_{n,k} = h^C(\mathbf{x}_{n,k}) + \eta^C_{n,k}, \tag{11}$$

where

$$h^C(\mathbf{x}_{n,k}) = \phi_{n,k} = \tan^{-1}(x_{n,k}, y_{n,k}). \tag{12}$$

The additive noise term $\eta^C_{n,k}$ is defined by

$$\eta^C_{n,k} \sim \mathcal{N}(\eta^C_{n,k}; \mathbf{0}, \sigma^2_{\phi_c}) \tag{13}$$

where σ_{ϕ_c} is the camera azimuth standard deviation.

In each case, the full set of observations at time n is given by $\mathbf{z}_n = [\mathbf{z}_{n,1}, \ldots, \mathbf{z}_{n,K}]^T$ corresponding to either the radar or camera, such that at each time-step $\mathbf{z}_{n,k} \in \{\mathbf{z}^C_{n,k}, \mathbf{z}^R_{n,k}\}$.

IV. PARAMETER LIKELIHOODS

This section presents a new result by deriving the sensor parameter likelihood, $\bar{\ell}_n(q_n|\mathbf{z}_n)$, used in Eq. (1b), for the MP based MTT method used in this paper, and summarises the known result for the SMC-PHD filter.

A. Particle-BP Algorithm

In order to use the SPA for marginalisation, it is assumed that the joint posterior $f(\mathbf{x}_n \mid \mathbf{z}_{1:n})$ can be seen as a product of M lower-dimensional factors,

$$f(\mathbf{x}_n \mid \mathbf{z}_{1:n}) \propto \prod_{m=1}^{M} \gamma_m(\mathbf{x}^{(m)}). \tag{14}$$

where each argument $\mathbf{x}^{(m)}$ comprises of a set of parameter vectors, $\mathbf{x}_{n,k}$, the set depending on the probabilistic models. This representation could also be drawn as a factor graph, Markov Random Field (MRF) or a Bayesian network [37]. In factor graphs, each variable $\mathbf{x}_k$ is represented with a variable node, and each factor $\gamma_m(\cdot)$ is represented with a factor node. A variable node is connected to a factor node if it is an argument of that factor. The factors may be complex and may need to be stretched into a larger number of factors in order to reduce the dimensionality of messages that will be passed amongst the nodes. The reduction in the message dimensions will result in lower computational complexity and improved scalability. A factor graph representation of the particle BP algorithm used in this work is shown in Fig. 5, with the following notation that is described in detail in the paragraphs below: $\tilde{f}$ represents the beliefs from iteration $n-1$; f represents the prediction step $f(\mathbf{y}_{n,k} \,|\, \mathbf{y}_{n-1,k})$ (see Eq. (16)); α is the marginal prediction (see (19)); υ is calculated through (22) and (23); β represents the correlation information used to initialise the association process (nodes a and b, messages ν and ς, and the exclusion enforcing

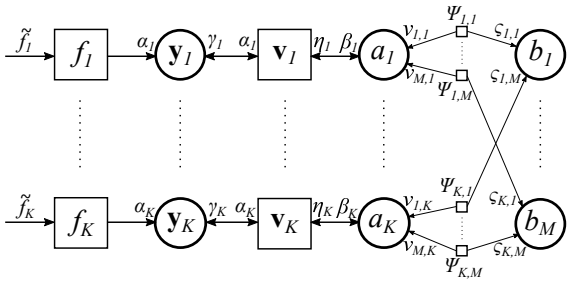

Fig. 5. Factor graph for the particle-BP algorithm.

function Ψ); η contains the result of the association step and γ represents the measurement update information. All messages are only *approximations* of the true messages because of the use of particle BP [13], [34]. In [13], the authors assume the sensor network is synchronised, and a parallelisation over multiple sensors is possible to update the target states. However, in this work, this is not possible as the sensors operate asynchronously. This parallelisation has been removed from the factor graph shown in Fig. 5.

By using MP, MTT methods with lower computational cost and better scalability can be developed [34]. In this section, the notation closely follows that of [13], [34]. To use a BP type algorithm for registration, a suitable sensor-parameter likelihood function is needed. An augmented target is defined as $\mathbf{y}_{n,k} = [\mathbf{x}_{n,k}, r_{n,k}]^T$, where $\mathbf{x}_{n,k}$ is a single target state, and $r_{n,k}$ is a binary existence variable. The prediction equation for $\mathbf{y}_n = \{\mathbf{y}_{n,k}\}_{k=1}^K$ is from Eq. (3a) with $\psi_n = \mathbf{y}_n$ and sensor configuration q':

$$p\left(\mathbf{y}_n \mid \mathbf{z}_{n-1}, q'\right) = \int f\left(\mathbf{y}_n \mid \mathbf{y}_{n-1}\right) p\left(\mathbf{y}_{n-1} \mid \mathbf{z}_{n-1}, q'\right) \mathrm{d}\mathbf{y}_{n-1} \tag{15}$$

where it is assumed the posterior can be factorised as

$$p\left(\mathbf{y}_{n-1} \mid \mathbf{z}_{n-1}, q'\right) = \prod_{k=1}^{K} p\left(\mathbf{y}_{n-1,k} \mid \mathbf{z}_{n-1}, q'\right), \tag{16}$$

as well as the target-state evolution, which does not depend on the sensor configuration:

$$f\left(\mathbf{y}_n \mid \mathbf{y}_{n-1}\right) = \prod_{k=1}^{K} f\left(\mathbf{y}_{n,k} \mid \mathbf{y}_{n-1,k}\right), \tag{17}$$

i.e. the joint target density is a product over all individual target densities. Following [13], [34], this is written as

$$p\left(\mathbf{y}_n \mid \mathbf{z}_{n-1}, q'\right) = \prod_{k=1}^{K} \alpha(\mathbf{y}_{n,k}\,;\, q') \tag{18}$$

where $\alpha(\mathbf{y}_{n,k}\,;\, \mathbf{z}_n, q')$ is the marginal prediction:

$$\begin{aligned} \alpha(\mathbf{y}_{n,k}\,;\, \mathbf{z}_n, q') = \sum_{r_{n-1,k}\in\{0,1\}} \int & f\left(\mathbf{y}_{n,k} \mid \mathbf{y}_{n-1,k}\right) \\ & \times p\left(\mathbf{y}_{n-1,k} \mid \mathbf{z}_{n-1}, q'\right) \mathrm{d}\mathbf{x}_{n-1,k} \end{aligned} \tag{19}$$

Introducing the target-oriented association variables, $\mathbf{a}_n$, the update equation for the BP implementation can be written as,

$$\begin{aligned} p\left(\mathbf{y}_n, \mathbf{a}_n \mid \mathbf{z}_n, \mathbf{z}_{1:n-1}, q'\right) &= p\left(\mathbf{z}_n \mid \mathbf{y}_n, \mathbf{a}_n, q'\right) \\ &\times \frac{p\left(\mathbf{a}_n \mid \mathbf{y}_n, \mathbf{z}_{1:n-1}, q'\right) p\left(\mathbf{y}_n \mid \mathbf{z}_{1:n-1}, q'\right)}{p\left(\mathbf{z}_n \mid \mathbf{z}_{1:n-1}, q'\right)} \end{aligned} \tag{20}$$

where $p\left(\mathbf{z}_n \mid \mathbf{y}_n, \mathbf{a}_n, q'\right)$ is the single-object association likelihood, $p\left(\mathbf{y}_n \mid \mathbf{z}_{1:n-1}, q'\right)$ contains the predicted target states from (18), and $p\left(\mathbf{z}_n \mid \mathbf{z}_{1:n-1}, q'\right) = \bar{\ell}_n(q' \mid \mathbf{z}_n)$ is the evidence term necessary for deriving the sensor-parameter likelihood function in Eq. (1b). A stretching process is used to reduce message dimensionality and computational complexity. Here, the random vector $\mathbf{b}_n$ is introduced, which is an alternative measurement-oriented association variable, and can be derived directly from $\mathbf{a}_n$ [13]. Stretching introduces loops into factor graphs, and these loops create instances where the messages or beliefs are no longer exact. However, in [34] it is shown the algorithm will still converge. By using $\mathbf{a}_n$ and $\mathbf{b}_n$, high-dimensional factors in the graph have been replaced with many lower-dimensional factors. Using stretching [13, Eq. (27)] and (20), it is shown:

$$\begin{aligned} &p(\mathbf{y}_n, \hat{\mathbf{a}}_n \mid \mathbf{z}_n, q') \ \propto \\ &\Psi(\hat{\mathbf{a}}_n) \frac{\prod_{k=1}^{K} v(\mathbf{y}_{n,k}, a_{n,k}\,;\, \mathbf{z}_n, q') \prod_{k=1}^{K} \alpha(\mathbf{y}_{n,k}\,;\, \mathbf{z}_n, q')}{p(\mathbf{z}_n \mid \mathbf{z}_{1:n-1}, q')} \end{aligned} \tag{21}$$

where $\hat{\mathbf{a}}_n = \{\mathbf{a}_n, \mathbf{b}_n\}$, $\Psi(\hat{\mathbf{a}}_n)$ is an "indicator" term that excludes all infeasible association events, (see [13, Eqs. 12 & 16] for complete details and caveats), and:

$$\begin{aligned} &v(\mathbf{x}_{n,k}, r_{n,k} = 1, a_{n,k}\,;\, \mathbf{z}_n,\, q') \\ &\qquad = \begin{cases} \frac{f(\mathbf{z}_{n,m} \mid \mathbf{x}_{n,k}, q')}{f_{FA}(\mathbf{z}_{n,m})} \frac{p_d}{\mu_c} & a_{n,k} = m \in M_n \\ 1 - p_d & a_{n,k} = 0 \end{cases} \end{aligned} \tag{22}$$

$$v(\mathbf{x}_{n,k}, r_{n,k} = 0, a_{n,k}\,;\, \mathbf{z}_n, q') = 1(a_{n,k}) \tag{23}$$

with $f_{FA}(\mathbf{z}_{n,m})$ representing the clutter distribution, μ_c is the mean number of false alarms, and M is the number of measurements, $m \in \{1, \ldots, M\}$. Note that following [13, Eqs. 12 & 24], there are normalisation terms $C(\mathbf{z})$ and $C(\mathbf{m})$ in Eq. (21); however, these are constant across the different filters with respect to different registration parameters q', as shown in [48]. Marginalising (21) over the joint space of all feasible association events, $\mathbf{a}_n$, and $\mathbf{y}_n$, gives the evidence:

$$\begin{aligned} p\left(\mathbf{z}_n \mid \mathbf{z}_{1:n-1}, q'\right) \propto \sum_{\mathbf{a}_n} \int \cdots \int \prod_{k=1}^{K} v(\mathbf{y}_{n,k}, a_{n,k}\,;\, \mathbf{z}_n, q') \\ \times \alpha(\mathbf{y}_{n,k}\,;\, q') \mathrm{d}\mathbf{y}_{n,1} \ldots \mathrm{d}\mathbf{y}_{n,k} \end{aligned} \tag{24}$$

which reduces, using the definition of $\beta(a_{n,k}\cdot)$ in [13, Eq. (31)], to:

$$\bar{\ell}_n(q' \mid \mathbf{z}_n) = p(\mathbf{z}_n \mid \mathbf{z}_{1:n-1}, q') \ \propto \ \sum_{\mathbf{a}_n} \prod_{k=1}^{K} \beta(a_{n,k}\,;\, \mathbf{z}_n, q') \tag{25}$$

where $\beta(a_{n,k}\,;\,\mathbf{z}_n, q')$ is defined by

$$\begin{aligned}&\beta(a_{n,k}\,;\,\mathbf{z}_n, q') = \\ &\qquad\sum_{r_{n,k}}\int v(\mathbf{y}_{n,k}, a_{n,k}\,;\,\mathbf{z}_n, q')\,\alpha(\mathbf{y}_{n,k}\,;\,\mathbf{z}_n, q')\,\mathrm{d}\mathbf{y}_{n,k}\end{aligned} \tag{26}$$

Note that $\beta(a_{n,k}\,;\,\mathbf{z}_n, q')$ can be interpreted as an approximation of the single-target association weights commonly found in the Probabilistic Data Association (PDA) and JPDA filters [16]. The final parameter likelihood equation in (25) can be implemented at the end of the correlation/association step inside the MTT process, where the β-terms have been pre-computed through MP operations. The likelihood in (25) *is not evaluated* through a MP operation, it merely exploits information already available as part of the offspring process.

The derived parameter likelihood is in the same form as that of the permanent of a matrix [49], [50]. These articles propose methods for directly computing the permanent, or approximations of the permanent. As the size of the matrix increases, the number of operations required to compute the permanent will increase exponentially. Because the number of targets and number of measurements are relatively small, the permanent will be computed directly in this case.

B. PHD Approach

This work will compare the MP approach to MTT with an SMC-PHD filter. The PHD filter is also a relatively recent development in this field. It was first developed in 2003 [51], with the SMC implementation first appearing in 2005 [52]. This filter propagates the first-order information of the target distribution (i.e. the mean number of targets), and assumes that both the predicted number of targets and the clutter cardinality are Poisson distributed.

This particle-based implementation of the PHD filter can also work explicitly with non-linearities, much like the MP approach. A direct application of typical SMC methods to propagate the PHD intensity would fail as it is not strictly a pdf, and the recursion used in the filter is not the standard Bayes recursion. Instead, the intensity function is represented by a large set of weighted random samples which are propagated over time using a generalised importance sampling and resampling strategy [52]. The number of particles in this set can be continually adapted, depending on the estimated number of targets in the surveillance region. It is noted that the main difference between this implementation and the MP approach is that the SMC-PHD filter uses a general particle distribution to represent all targets in the state space, rather than having N particles specifically for each individual target.

The parameter likelihood for the PHD filter is derived in [42], and for a given sensor configuration q' is,

$$\begin{aligned}&\bar{\ell}_n(q'\,|\,\mathbf{z}_n) = \\ &\frac{\prod_{z\in\mathbf{z}}\left[\mu_{c,n}\left(z\right) + \int_{\mathcal{X}} p_d\left(\mathbf{x}\right) g_n\left(z\,|\,\mathbf{x}, q'\right)\mu_{n|n-1}\left(\mathrm{d}\mathbf{x}\,|\,q'\right)\right]}{\exp\left[\int_{\mathcal{Z}}\mu_{c,n}\left(z\right)\mathrm{d}z + \int_{\mathcal{X}} p_d\left(\mathbf{x}\right)\mu_{n|n-1}\left(\mathrm{d}\mathbf{x}\,|\,q'\right)\right]}\end{aligned} \tag{27}$$

where $p_d\left(\mathbf{x}\right)$ is the probability of detection, $g_n\left(z\,|\,\mathbf{x}, q'\right)$ is the single-object likelihood, $\mu_{c,n}\left(z\right)$ is the clutter intensity, $\mu_{n|n-1}\left(\mathrm{d}\mathbf{x}\,|\,q'\right)$ is the predicted intensity. This likelihood function is implemented as a part of the PHD filter update step. This function will simplify as the integrals become summations of all components for one measurement, i.e. a sum of the corresponding component weights.

V. Performance Metrics

In order to compare the two types of filter for performing simultaneous tracking and registration, the Generalized Optimal Sub-Pattern Assignment (GOSPA) metric [53] will be used. The GOSPA distance is made up of a cardinality error and a localisation error between two sets X and Y with cardinalities m and n respectively. It generalises the Optimal Sub-Pattern Assignment (OSPA) metric [54] by including an additional parameter $\hat{\alpha}$, enabling a choice of cardinality mismatch cost, hence giving a sum of localisation errors for detected targets, and penalising missed and false targets. This closely follows traditional MTT performance assessment metrics. The GOSPA metric is given by [53, Eq. (1)]

$$d_p^{(c,\alpha)}(X,Y) = \left[\min_{\pi \in \Pi_n} \sum_{i=1}^{m} d^{(c)}(x_i, y_{\pi(i)})^p + \frac{c^p}{\hat{\alpha}}(n-m) \right]^{\frac{1}{p}}, \tag{28}$$

using an order parameter p, and a cut-off distance c. Here, the distance function $d^{(c)}(x,y) = \min(d(x,y), c)$ is an appropriate distance measure, e.g. the Euclidean distance, cut off at c, and Π_n denotes the set of all possible permutations of the numbers $1, \ldots, n$. As the order parameter increases, the metric penalises estimates that are further away from the ground truth more harshly. From [54, Sec. III-D], $p = 2$ is a good practical choice for the order parameter, as it usually gives smoother distance curves, and is consistent with other metrics that use a p-th order average construction. The cut-off distance c determines the trade-off between penalising cardinality errors as opposed to localisation errors. For all GOSPA results shown, $\hat{\alpha} = 2$ as recommended in [53], the cut-off parameter of $c = 100$ m and an order parameter $p = 2$ will be used.

The algorithms will also be compared in terms of computation time per iteration. All simulations have been run on a desktop PC containing an Intel Core i7-6700K CPU with a clock speed of 4 GHz and 16 gigabytes of RAM. Because each of the sensor configurations to be evaluated are independent of one another, it is possible to parallelise the filtering process, further improving the computational efficiency.

VI. Simulations

Previous work that uses this type of hierarchical model [5] contains a grid-based method [44, pp. 9] to represent the high-level process in practice. Particles were evenly distributed on this grid to perform a consistent parameter test, and to remove the need for particle resampling. This method has a drawback; in that outliers that are far from the true parameter values will be continually tested unnecessarily and contribute little to the overall estimation. We introduce a resampling strategy into our simulations, where if the effective sample size is below a given threshold, the sensor configurations are resampled. Both sets of simulations use 324 particles, which will be initialised uniformly across the appropriate parameter space, as shown in Fig. 6. The parameters used in the low-level tracking process are given in Table I and are consistent across all scenarios. The simulated target trajectories are also consistent, and an overview of these is shown in Fig. 7.

The GOSPA results shown in Table III and Table IV later in the paper are based on three different measurement noise combinations; low, medium and high. The values for these measurement noises are shown in Table II.

TABLE I

TRACKING PARAMETERS

Quantity	**Symbol**	**Value**
Survival Probability	p_s	0.95
Gating Threshold	τ_{gate}	99%
Pruning Threshold	τ_{prune}	0.001
Extraction Threshold	$\tau_{extract}$	0.5
False Alarm Rate	λ_r, λ_c	2, 5
Birth Intensity	μ_b	0.01
Acceleration Noise	q	1 ms^{-2}
Particles per Target	N	1000
Maximum Number of Targets	K	7

TABLE II

MEASUREMENT NOISE LEVELS

Noise Level	σ_{r_r}	σ_{ϕ_r}	σ_{ϕ_c}
Low Noise	5 m	0.05°	0.01°
Medium Noise	10 m	0.1°	0.03°
High Noise	20 m	0.2°	0.05°

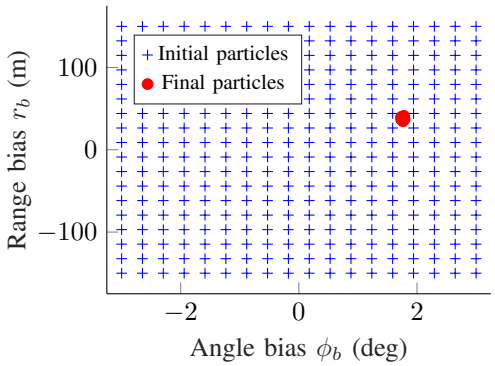

Fig. 6. An example of the sensor configurations represented by a particle distribution in the high-level process for the homogeneous scenario. Particles are initialised uniformly between $r_b = [-150\,\text{m} \rightarrow 150\,\text{m}], \phi_b = [-3° \rightarrow 3°]$, and converge towards the correct biases over time.

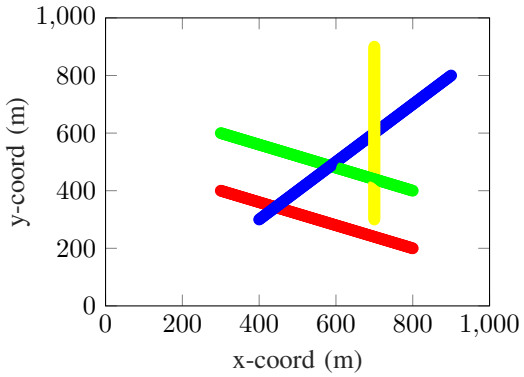

Fig. 7. Simulated target trajectories for all scenarios and sensor setups. Each line represents one of the four different target trajectories.

A. *Homogeneous Network*

For this scenario, we consider the sensor setup shown in Fig. 1 which contains two radars observing a common surveillance region. The radars are physically separated by a number of kilometres, in fixed and known locations, but there is some uncertainty in their relative orientation as shown in Fig. 3(a). Modern radar systems typically have a much smaller down-range uncertainty than cross-range uncertainty. The down-range uncertainty is determined by how fast the system can sample the received return signal, which could be in the order of a few metres. Cross-range uncertainty is determined by the width of the radar beam when it has been projected onto the ground plane. This distance could be in the order of hundreds of metres. By using the down-range measurement in one radar to correct the cross-range measurement in the other radar, we could drastically reduce the overall uncertainty in target location. It is desired to estimate both the bias in range and the bias in azimuth, alongside the multiple target states. For this scenario, the true biases simulated are $r_b = 30\,\mathrm{m}$ and $\phi_b = 2°$.

We first demonstrate the accuracy and stability of results over a number of Monte-Carlo (MC) runs. The results plotted in Fig. 8 show that for the homogeneous scenario described above, both methods provide stable GOSPA results, even if a low number of runs are included. Therefore, all further results presented have been averaged over 100 MC runs, which Fig. 8 shows to be adequate.

From Fig. 9a and Fig. 9b, the proposed method of simultaneous tracking and registration (black dash-dotted plot) outperforms the use of a single radar (red dashed plot), but as expected, does not reach the optimal performance of having a perfectly registered set of sensors (solid green plot). The unregistered set of sensors (dotted blue plot) performs much worse; this underlines the importance of taking the registration problem into account while attempting to fuse information from multiple sensors. At the end of the scenario, the GOSPA distance for the PHD approach is $64.2\,\mathrm{m}$ and $54.2\,\mathrm{m}$ for the MP approach, giving the MP approach a performance gain of around 10% over the PHD approach.

In terms of the parameter estimation results in Fig. 10, there is less variation in the estimated range value using the PHD approach than with the MP approach – explained by recalling that the PHD approach does not include data association. For the vast majority of the scenario, the MP approach is within $0.07°$ of the true angle bias as

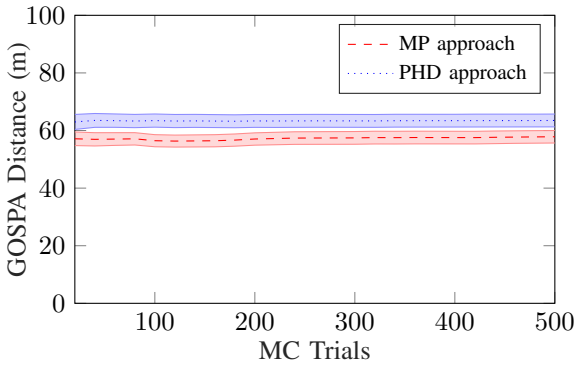

Fig. 8. Average GOSPA Distance over the number of Monte-Carlo runs included.

shown in Fig. 10b. The PHD approach took $0.781\,\mathrm{s}$ per iteration on average, with the MP approach marginally slower at $1.086\,\mathrm{s}$ per iteration.

The results involving different probabilities of detection are shown in Fig. 11. As the probability of detection increases from 0.8 through to 0.99, it can be seen that the GOSPA distance decreases and the tracking accuracy continues to improve as expected. In Fig. 11b and Fig. 11c, there is only a small change in the overall average of the estimated parameters with p_d; however the overall spread or variation in the result becomes smaller.

For the different noise variations and corresponding results in Table III, it can be seen that the MP approach is more accurate in the low noise cases, across all of the probabilities of detection. In the high noise scenarios, both methods have largely deteriorated and give poor tracking accuracy; there is no discernible difference between them. At the medium noise level, the proposed MP approach deteriorates more rapidly than the PHD approach. This may be due to the PHD approach not taking the data association problem in to account. As the MP approach makes a hard decision through the use of correlation, high levels of noise may generate measurements that lie outside the gating threshold, and therefore will not be associated to a target.

B. Heterogeneous Network

Now consider a sensor setup where a radar and a camera are co-located on the same static platform, as described in Fig. 3(b) in Sect. I. Cameras typically have a much higher update rate than radars, and this is exploited to maintain track estimates more frequently. For the simulated scenario, the high update rate is important, as if sensors operate too slowly, track resolution could be lost and wrong measurement-to-track associations could be made. Here, it is desired to estimate the relative angular bias $q_n = \phi_b = 2°$ between the sensors, alongside the multiple target states.

As shown in Fig. 12a, both the PHD approach and the MP approach perform better than their respective single radar cases in terms of tracking accuracy, but not as well as the correct registration cases. The proposed MP approach is more accurate than the PHD approach for the low noise cases. At the end of the scenario, the GOSPA distance for MP is $47.8\,\mathrm{m}$ and $72.6\,\mathrm{m}$ for the PHD, giving a more substantial performance gain at around 25%. The parameter estimation results in Fig. 13 are very comparable with the MP approach $0.05°$ away from the true value,

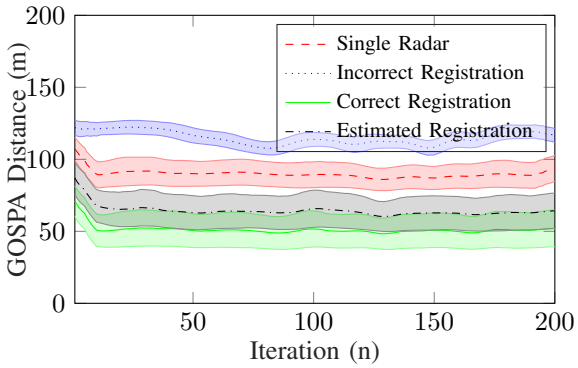

(a) PHD approach

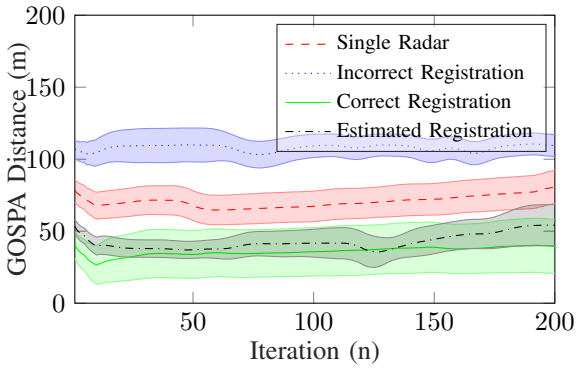

(b) MP approach

Fig. 9. Homogeneous sensors, $p_d = 0.99$

and the PHD approach $0.06°$ away after the first 100 iterations. The PHD approach took more time to reach accurate parameter estimation, and the MP method provided a more consistent estimate over time. The PHD approach took $1.203\,\mathrm{s}$ per iteration on average, with the MP approach slower at $1.530\,\mathrm{s}$ per iteration.

When considering the different probabilities of target detection, in Fig. 14, it can again be seen that the GOSPA distance decreases as p_d increases. For lower probabilities of detection, the MP method provides a more accurate average estimate of the angle bias between the radar and the camera. A full breakdown of the results for the different p_d values, and for the different noise levels for the heterogeneous scenario are given in Table IV. We see similar behaviour to that of the homogeneous case; the proposed MP approach performs best in low measurement noise cases, the MP method deteriorates more quickly at medium noise cases, and both methods perform badly with high noise.

VII. Conclusions

From the comprehensive results, the proposed MP approach has shown to provide more accurate target tracking and sensor registration estimation than that of the RFS approach in low measurement noise cases. When considering the low noise cases, the proposed MP approach performs approximately 17% more accurately in terms of the GOSPA metric, than the RFS approach. All of the results highlight the importance of having an accurately registered set of

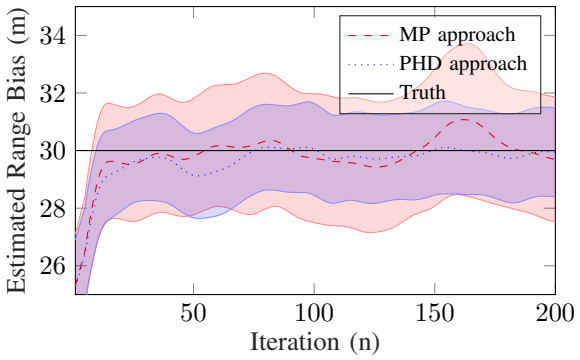

(a) Range r_b estimation

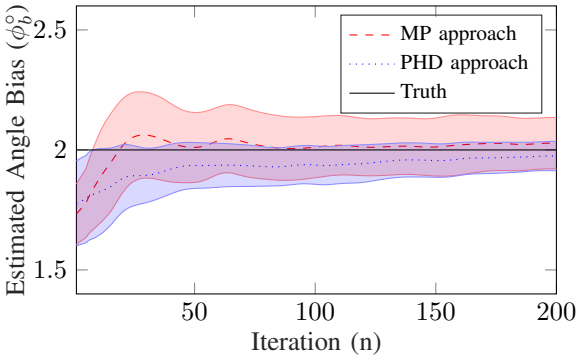

(b) Angle ϕ_b estimation

Fig. 10. Registration parameter estimation, homogeneous sensors, $p_d = 0.99$

TABLE III
HOMOGENEOUS NETWORK, AVERAGE GOSPA DISTANCES AT $n = 200$

	p_d	0.80			0.85			0.90			0.95			0.99		
	Noise	Low	Med	High	Low	Med	High	Low	Med	High	Low	Med	High	Low	Med	High
Single Radar	PHD	**144**	164	202	**135**	155	197	**122**	144	193	**101**	132	189	**94**	126	187
	MP	**120**	192	200	**117**	189	199	**106**	186	197	**102**	178	195	**80**	167	186
Incorrect	PHD	**152**	191	209	**145**	166	207	**137**	150	203	**117**	136	197	**117**	134	197
	MP	**155**	199	205	**144**	195	203	**139**	191	203	**128**	188	208	**109**	182	203
Proposed	PHD	**134**	164	183	**129**	145	195	**115**	133	191	**73**	98	170	**64**	95	151
	MP	**107**	189	199	**101**	182	195	**83**	170	179	**69**	149	158	**54**	136	154
Correct	PHD	**130**	150	164	**121**	140	181	**103**	130	178	**62**	82	158	**52**	78	139
	MP	**97**	183	194	**87**	180	190	**62**	156	176	**58**	140	165	**39**	134	150

sensors when performing fusion, as tracking accuracy can dramatically reduce when the registration is incorrect. When considering the high measurement noise level, both methods deteriorate and perform badly as expected. For the medium noise case, the MP method deteriorates more rapidly than the RFS approach due to issues with the correlation and association steps. The noisy measurements, when used in the correlation step in the MP method, may lie outside the gating threshold and therefore not be associated to a target and reduce the overall accuracy of

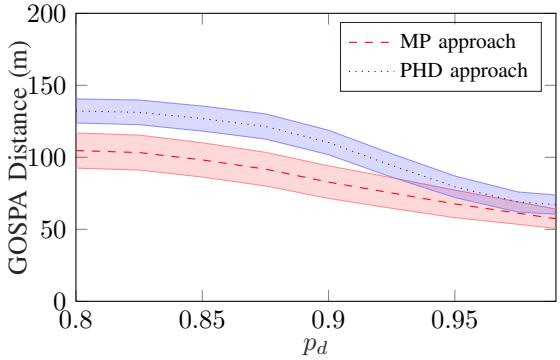

(a) GOSPA Distance

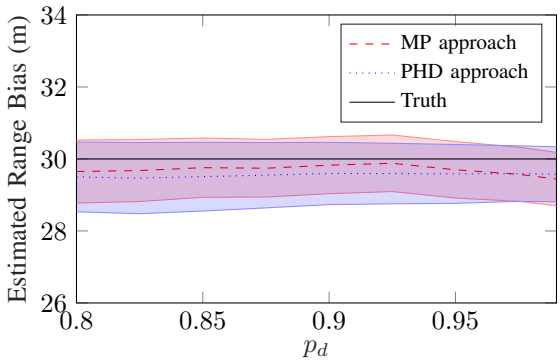

(b) Range r_b estimation

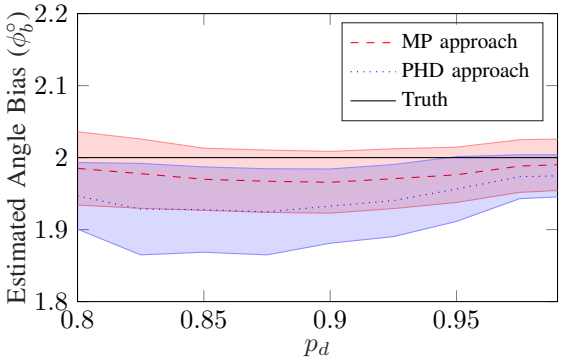

(c) Angle ϕ_b estimation

Fig. 11. Varying p_d results, homogeneous sensors, average value at $n = 200$, low measurement noise values.

the target tracking.

Previous works in this field have shown that the MP for MTT algorithm should be more computationally efficient than that of the PHD filter and its variants; so far we have not been able to recreate this result, and our implementation of the MP approach continues to run approximately 20% slower than the RFS approach.

Currently, the formulation of the parameter likelihood is based around the hierarchical model, or single-cluster method approach, where the sensor registration and fusion problems are connected. The parameter likelihood used in this work is evaluated using information already available from the MTT algorithm. Some future work could

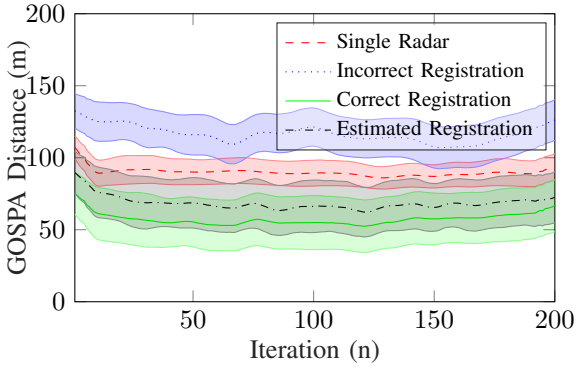

(a) PHD approach

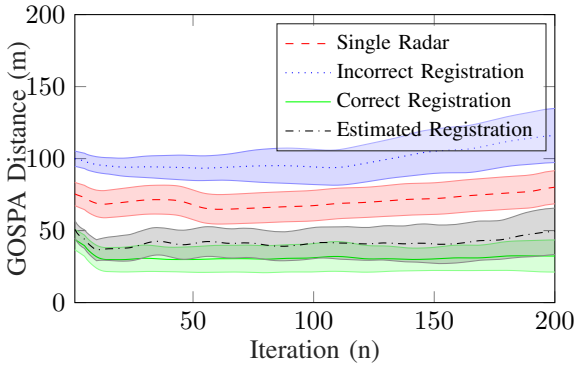

(b) MP approach

Fig. 12. Heterogeneous sensors, $p_d = 0.99$

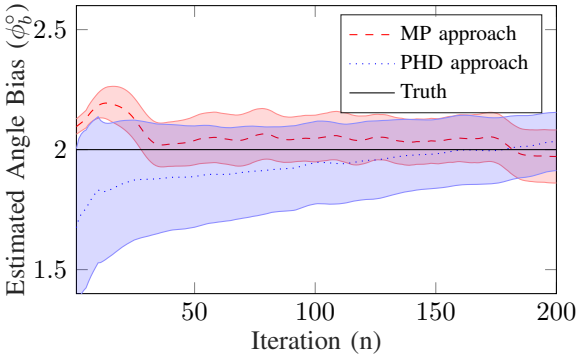

Fig. 13. Angular bias ϕ_b estimation, heterogeneous sensors, $p_d = 0.99$

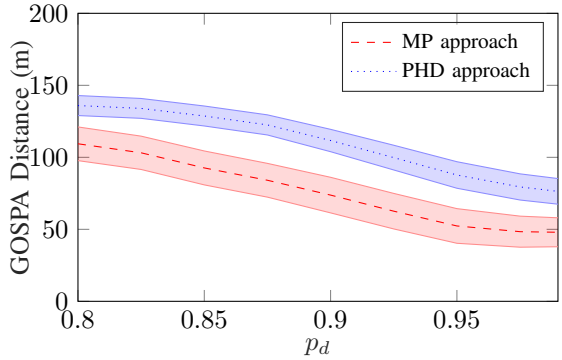

(a) GOSPA Distance

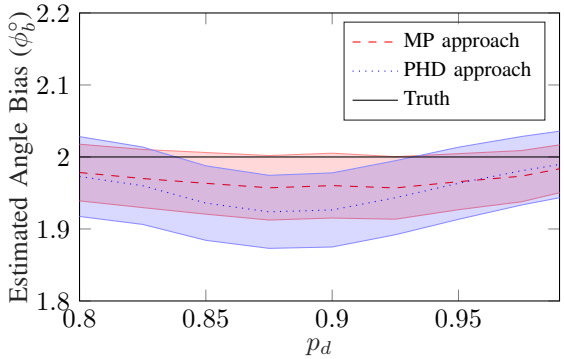

(b) Angle ϕ_b estimation

Fig. 14. Varying p_d results, heterogeneous sensors, average value at $n = 200$, low measurement noise values.

TABLE IV
HETEROGENEOUS NETWORK, AVERAGE GOSPA DISTANCES AT $n = 200$

	p_d	0.80			0.85			0.90			0.95			0.99		
	Noise	Low	Med	High	Low	Med	High	Low	Med	High	Low	Med	High	Low	Med	High
Single Radar	PHD	**144**	164	202	**135**	155	197	**122**	144	193	**101**	132	189	**94**	126	187
	MP	**120**	192	200	**117**	189	199	**106**	186	197	**102**	178	195	**80**	167	186
Incorrect	PHD	**170**	180	219	**164**	173	213	**155**	167	211	**135**	151	203	**126**	142	197
	MP	**189**	216	222	**175**	211	222	**160**	207	220	**140**	204	218	**116**	193	210
Proposed	PHD	**137**	152	192	**130**	145	186	**116**	136	182	**86**	116	175	**73**	103	168
	MP	**114**	189	197	**91**	187	194	**79**	182	196	**49**	174	191	**48**	161	182
Correct	PHD	**127**	141	181	**118**	132	177	**108**	124	174	**79**	105	165	**67**	93	157
	MP	**101**	179	193	**84**	177	192	**56**	180	193	**44**	171	187	**32**	159	181

include the use of other message passing approximations such as the Bethe permanent [55] to evaluate this parameter likelihood in a message passing framework.

REFERENCES

[1] W. Koch, *Tracking and Sensor Data Fusion: Methodological Framework and Selected Applications*, 1st ed. Berlin: Springer Verlag, 2014.

[2] G. Stimson, *Stimson's Introduction to Airborne Radar*, 3rd ed., H. Griffiths, C. Baker, and D. Adamy, Eds. SciTech Publishing, 2014.

[3] C. S. Lee, D. Clark, and J. Salvi, "SLAM with Dynamic Targets via Single-Cluster PHD Filtering," *IEEE Journal of Selected Topics in Signal Processing*, vol. 7, no. 3, pp. 543–552, 2013.

[4] I. Schlangen, J. Franco, J. Houssineau, W. Pitkeathly, D. Clark, I. Smal, and C. Rickman, "Marker-less Stage Drift Correction in Super-Resolution Microscopy Using the Single-Cluster PHD Filter," *IEEE Journal of Selected Topics in Signal Processing*, vol. 10, no. 1, pp. 193–202, 2016.

[5] I. Schlangen, V. Bharti, E. Delande, and D. E. Clark, "Joint multi-object and clutter rate estimation with the single-cluster PHD filter," in *IEEE 14th International Symposium on Biomedical Imaging (ISBI 2017)*. Melbourne, Australia: IEEE, 2017, pp. 1087 – 1091.

[6] G. Soldi, D. Gaglione, F. Meyer, F. Hlawatsch, P. Braca, A. Farina, and M. Z. Win, "Heterogeneous Information Fusion for Multitarget Tracking using the Sum-Product Algorithm," in *IEEE International Conference on Acoustics, Speech and Signal Processing (ICASSP)*. Brighton, UK: IEEE, 2019.

[7] G. Soldi, F. Meyer, P. Braca, and F. Hlawatsch, "Self-Tuning Algorithms for Multisensor-Multitarget Tracking Using Belief Propagation," *IEEE Transactions on Signal Processing*, vol. 67, no. 15, pp. 3922 – 3937, 2019.

[8] E. Taghavi, R. Tharmarasa, T. Kirubarajan, Y. Bar-Shalom, and M. Mcdonald, "A Practical Bias Estimation Algorithm for Multisensor-Multitarget Tracking," *IEEE Transactions on Aerospace and Electronic Systems*, vol. 52, no. 1, pp. 2 – 19, 2016.

[9] D. Huang, H. Leung, and E. Bosse, "A Pseudo-Measurement Approach to Simultaneous Registration and Track Fusion," *IEEE Transactions on Aerospace and Electronic Systems*, vol. 48, no. 3, pp. 2315 – 2331, 2012.

[10] J. Williams and R. Lau, "Approximate evaluation of marginal association probabilities with belief propagation," *IEEE Transactions on Aerospace and Electronic Systems*, vol. 50, no. 4, pp. 2942 – 2959, 2014.

[11] X. Lin, Y. Bar-Shalom, and T. Kirubarajan, "Exact Multisensor Dynamic Bias Estimation with Local Tracks," *IEEE Transactions on Aerospace and Electronic Systems*, vol. 40, no. 2, pp. 576 – 590, 2004.

[12] D. Cormack, I. Schlangen, J. R. Hopgood, and D. E. Clark, "Joint Registration and Fusion of an Infra-Red Camera and Scanning Radar in a Maritime Context," *IEEE Transactions on Aerospace and Electronic Systems*, 2019.

[13] F. Meyer, P. Braca, P. Willett, and F. Hlawatsch, "A Scalable Algorithm for Tracking an Unknown Number of Targets Using Multiple Sensors," *IEEE Transactions on Signal Processing*, vol. 65, no. 13, pp. 3478–3493, 2017.

[14] D. Cormack and J. R. Hopgood, "Message Passing for Joint Registration and Tracking in Multistatic Radar," in *Sensor Signal Processing for Defence (SSPD) 2019*. Brighton, UK: IEEE, 2019.

[15] ——, "Sensor Registration and Tracking from Heterogeneous Sensors with Belief Propagation," in *22nd International Conference on Information Fusion (FUSION)*. Ottawa, CA: IEEE, 2019.

[16] Y. Bar-Shalom, P. K. Willett, and X. Tian, *Tracking and Data Fusion: A Handbook of Algorithms*. Storrs, CT, USA: YBS Publishing, 2011.

[17] B. Ristic, D. Clark, and N. Gordon, "Calibration of Multi-Target Tracking Algorithms Using Non-Cooperative Targets," *IEEE Journal of Selected Topics in Signal Processing*, vol. 7, no. 3, pp. 390–398, 2013.

[18] G. Mirzaei, M. M. Jamali, J. Ross, P. V. Gorsevski, and V. P. Bingman, "Data Fusion of Acoustics, Infrared and Marine Radar for Avian Study," *IEEE Sensors Journal*, vol. 15, no. 11, pp. 6625–6632, 2015.

[19] S. Maresca, P. Braca, J. Horstmann, and R. Grasso, "Maritime Surveillance Using Multiple High-Frequency Surface-Wave Radars," *IEEE Transactions on Geoscience and Remote Sensing*, vol. 52, no. 8, pp. 5056 – 5071, 2014.

[20] H. Karniely and H. Siegelmann, "Sensor registration using neural networks," *IEEE Transactions on Aerospace and Electronic Systems*, vol. 36, no. 1, pp. 85–101, 2000.

[21] N. Schneider, F. Piewak, C. Stiller, and U. Franke, "RegNet: Multimodal sensor registration using deep neural networks," in *2017 IEEE Intelligent Vehicles Symposium*. Los Angeles, CA: IEEE, 2017, pp. 1803–1810.

[22] G. Marcus, "Deep Learning: A Critical Appraisal," *ArXiv e-prints, ArXiv: 1801.00631*, pp. 1–27, 2018. [Online]. Available: https://arxiv.org/abs/1801.00631

[23] P. Domingos, *The Master Algorithm: How the Quest for the Ultimate Learning Machine Will Remake Our World*, 1st ed. London, UK: Allen Lane, 2015.

[24] M. Uney, B. Mulgrew, and D. E. Clark, "A Cooperative Approach to Sensor Localisation in Distributed Fusion Networks," *IEEE Transactions on Signal Processing*, vol. 64, no. 5, pp. 1187–1199, 2016.

[25] ——, "Latent Parameter Estimation in Fusion Networks Using Separable Likelihoods," *IEEE Transactions on Signal and Information Processing over Networks*, vol. 4, no. 4, pp. 752 – 768, 2018.

[26] T. Fortmann, Y. Bar-Shalom, and M. Scheffe, "Multi-Target Tracking using Joint Probabilistic Data Association," in *19th IEEE Conference on Decision and Control including the Symposium on Adaptive Processes*. Albuquerque, NM, USA: IEEE, 1980, pp. 807–812.

[27] D. B. Reid, "An Algorithm for Tracking Multiple Targets," *IEEE Transactions on Automatic Control*, vol. 24, no. 6, pp. 843–854, 1979.

[28] B.-N. Vo, M. Mallick, Y. Bar-Shalom, S. Coraluppi, R. Osborne, R. Mahler, and B.-T. Vo, "Multitarget Tracking," in *Wiley Encyclopedia of Electrical and Electronics Engineering*. American Cancer Society, 2015, pp. 1–15.

[29] R. Mahler, *Statistical Multisource-Multitarget Information Fusion*. Norwood, MA: Artech House, 2007.

[30] B.-N. Vo and W.-K. Ma, "The Gaussian Mixture Probability Hypothesis Density Filter," *IEEE Transactions on Signal Processing*, vol. 54, no. 11, pp. 4091–4104, 2006.

[31] R. Mahler, "PHD Filters of Higher Order in Target Number," *IEEE Transactions on Aerospace and Electronic Systems*, vol. 43, no. 4, pp. 1523–1543, 2007.

[32] B.-N. Vo, B.-T. Vo, and D. Phung, "Labeled Random Finite Sets and the Bayes Multi-Target Tracking Filter," *IEEE Transactions on Signal Processing*, vol. 62, no. 24, pp. 6554 – 6567, 2014.

[33] B.-N. Vo, B.-T. Vo, and H. G. Hoang, "An Efficient Implementation of the Generalized Labeled Multi-Bernoulli Filter," *IEEE Transactions on Signal Processing*, vol. 65, no. 8, pp. 1975 – 1987, 2017.

[34] F. Meyer, T. Kropfreiter, J. L. Williams, R. A. Lau, F. Hlawatsch, P. Braca, and M. Z. Win, "Message Passing Algorithms for Scalable Multitarget Tracking," *Proceedings of the IEEE*, vol. 106, no. 2, pp. 221–259, 2018.

[35] R. Kalman, "A New Approach to Linear Filtering and Prediction Problems," *ASME Journal of Basic Engineering*, vol. 82, no. 1, pp. 35–45, 1960.

[36] M. S. Arulampalam, S. Maskell, N. Gordon, and T. Clapp, "A tutorial on particle filters for online nonlinear/non-Gaussian Bayesian tracking," *IEEE Transactions on Signal Processing*, vol. 50, no. 2, pp. 174–188, 2002.

[37] F. Kschischang, B. Frey, and H.-A. Loeliger, "Factor graphs and the sum-product algorithm," *IEEE Transactions on Information Theory*, vol. 47, no. 2, pp. 498 – 519, 2001.

[38] H. W. Kuhn, "The Hungarian Method for the Assignment Problem," *Naval Research Logistics Quarterly*, vol. 2, pp. 83–97, 1955.

[39] D. Bertsekas, "A New Algorithm for the Assignment Problem," *Mathematical Programming*, vol. 21, no. 1, pp. 152–171, 1981.

[40] T. Kurien, "Issues in the Design of Practical Multitarget Tracking Algorithms," in *Multitarget-Multisensor Tracking: Advanced Applications*, Y. Bar-Shalom, Ed. Norwood, MA: Artech House, 1990, ch. 3, pp. 43 – 83.

[41] D. Musicki, R. Evans, and S. Stankovic, "Integrated probabilistic data association," *IEEE Transactions on Automatic Control*, vol. 39, no. 6, pp. 1237 – 1241, 1994.

[42] A. Swain, "Group and extended target tracking with the probability hypothesis density filter," Ph.D. dissertation, Heriot-Watt University, 2013.

[43] I. Schlangen, "Multi-object filtering with second-order moment statistics," Ph.D. dissertation, Heriot-Watt University, 2017.

[44] B. Ristic, S. Arulampalam, and N. Gordon, *Beyond the Kalman Filter: Particle Filters for Tracking Applications*, 1st ed. Boston, MA: Artech House, 2004.

[45] A. Doucet, N. de Freitas, and N. Gordon, *Sequential Monte Carlo Methods in Practice*. New York, NY: Springer-Verlag, 2001.

[46] T. Li, M. Bolic, and P. M. Djuric, "Resampling Methods for Particle Filtering: Classification, Implementation and Strategies," *IEEE Signal Processing Magazine*, vol. 32, no. 3, pp. 70–86, 2015.

[47] X. Rong-Li and V. Jilkov, "Survey of maneuvering target tracking. Part I. Dynamic models," *IEEE Transactions on Aerospace and Electronic Systems*, vol. 39, no. 4, pp. 1333 – 1364, 2003.

[48] D. Cormack and J. R. Hopgood, "The Formulation of the Parameter Likelihood: A supplement supporting the publication "Message Passing and Hierarchical Models for Simultaneous Tracking and Registration"," *IEEE Transactions on Aerospace and Electronic Systems*, 2020.

[49] B. Huang and T. Jebara, "Approximating the Permanent with Belief Propagation," *ArXiv e-prints, ArXiv:0908.1769*, 2009.

[50] M. Chertkov and A. B. Yedidia, "Approximating the Permanent with Fractional Belief Propagation," *Journal of Machine Learning Research*, vol. 14, pp. 2029 – 2066, 2013.

[51] R. Mahler, "Multitarget Bayes filtering via first-order multitarget moments," *IEEE Transactions on Aerospace and Electronic Systems*, vol. 39, no. 4, pp. 1152–1178, 2003.

[52] B.-N. Vo, S. Singh, and A. Doucet, "Sequential Monte Carlo methods for multitarget filtering with random finite sets," *IEEE Transactions on Aerospace and Electronic Systems*, vol. 41, no. 4, pp. 1224 – 1245, 2005.

[53] A. S. Rahmathullah, A. F. Garcia-Fernandez, and L. Svensson, "Generalized optimal sub-pattern assignment metric," in *20th International Conference on Information Fusion*. Xi'an, China: IEEE, 2017.

[54] D. Schuhmacher, B.-T. Vo, and B.-N. Vo, "A Consistent Metric for Performance Evaluation of Multi-Object Filters," *IEEE Transactions on Signal Processing*, vol. 56, no. 8, pp. 3447–3457, 2008.

[55] J. L. Williams and R. A. Lau, "Multiple Scan Data Association by Convex Variational Inference," *IEEE Transactions on Signal Processing*, vol. 66, no. 8, pp. 2112 – 2127, 2018.

David Cormack received the M.Eng. degree in electrical and electronic engineering with distinction from Heriot-Watt University, Edinburgh, UK in 2016. He is currently working towards the Ph.D. degree in signal processing, awarded jointly by Heriot-Watt University and The University of Edinburgh. He has completed a number of internships at Leonardo MW Ltd, Edinburgh, and they now sponsor his Ph.D. degree. His research interests include radar signal processing, target detection, multiple target tracking, sensor fusion and sensor calibration.

James R. Hopgood (M'02) received the Ph.D. degree from the University of Cambridge, U.K., in 2001. He was a Research Fellow at Queens' College and the Signal Processing Laboratory in Cambridge until 2004. He has since been at the University of Edinburgh, Scotland, where he is currently Director of Electronics and Electrical Engineering and a Senior Lecturer in the School of Engineering, and is a member of the Institute for Digital Communications. His research projects span a number of applications in statistical signal and image processing. He has been Editor-in-Chief for the IET Journal of Signal Processing since 2011.